Electronic Supplementary Material (ESI) for Physical Chemistry Chemical Physics.
This journal is © the Owner Societies 2017

Journal Name

ARTICLE TYPE

Cite this: DOI: 10.1039/xxxxxxxxxx

ESI: Understanding the interactions between sebum triglycerides and water: a molecular dynamics simulation study

Anna Sofia Tascini,[a] Massimo Noro,[b] Rongjun Chen,[c] John M. Seddon[a] and Fernando Bresme[a]

Received Date
Accepted Date

DOI: 10.1039/xxxxxxxxxx

www.rsc.org/journalname

Electronic supplementary information of Understanding the interactions between sebum triglycerides and water: a molecular dynamics simulation study

1 Input configurations

We consider four different configurations to investigate the properties of the sebum triglyceride (TG) and the mechanisms of interaction of TG with water. Fig. S1 shows the four input configurations employed (from 1 to 4): bulk TG, TG-air interface, TG-water interface and a TG monolayer at the air-water interface. Fig. S1-1 displays a box of 512 triglycerides equilibrated for 80 ns, as described in the main paper. This box is duplicated along the x and y directions to generate the configuration employed in the simulation. A vacuum region was added along the z axis to generate two TG-air interfaces which are shown in Fig. S1-2. In the TG-water interfaces (see Fig. S1-3) the void space was filled with 32126 water molecules. Starting from an equilibrated TG-water interface, the monolayer configuration, displayed in Fig. S1-4, is obtained by selecting all the TG molecules with the central carbon atom of the glycerol group (C2) close to the first water interface along z, such that the distance between C2 and the interface was $\leq 1\,\mathrm{nm}$. The resulting monolayer consists of 122 TG molecules whose glycerol group was partially immersed in a water film with 9085 water molecules. The other surface of the water film was instead left free from TG. The main simulation parameters are summarised in Tab. S1. *NPT* on z denotes the fact that the pressure barostat is applied along the z axis, while the area of the simulation box in the Xy plane is kept constant.

2 Bulk TG

2.1 Shape classification

Four representative shapes can be used to describe the conformation of a TG molecule:

1. **Propeller (Pr)**: the three angles are uniformly distributed around an average value of 120° (also called Y-shape in previous analysis[1])
2. **Tuning fork (TF)**: two opposite chains are pointing in the same direction and the third one in the opposite direction
3. **Chair (Ch)**: two adjacent chains are pointing in the same direction and the third one in the opposite direction
4. **Trident (Tr)**: the three chains are pointing in the same direction

We defined four criteria to link the four shapes, described above, to the energetically favourable regions of TG conformations, expressed in terms of the three angle θ_{12}, θ_{23} and θ_{13}, defined in the main paper.

The criteria were defined as follows.

1. **Pr:** $(75 < \theta_{12} < 165)$ & $(75 < \theta_{23} < 165)$ & $(75 < \theta_{13} < 165)$
2. **TF:** $(95 < \theta_{12} < 180)$ & $(95 < \theta_{23} < 180)$ & $(0 < \theta_{13} < 75)$
3. **Ch:**
$$\begin{cases} (0 < \theta_{12} < 75)\ \&\ (95 < \theta_{23} < 180)\ \&\ (95 < \theta_{13} < 180) \\ (95 < \theta_{12} < 180)\ \&\ (0 < \theta_{23} < 75)\ \&\ (95 < \theta_{13} < 180) \end{cases}$$
4. **Tr:** otherwise.

The trident region includes all those conformation where at least two of the angle are lower than 95°. We expect, in fact, that the presence of the double bond will result in a wide trident configuration, where one of the three angle might be higher than 95°.

We show in Fig.S2 the regions assigned to the 4 conformations with different colours: blue for the *propeller*, red for the *tuning fork* and magenta for the *chair*. The region assigned to the trident has been left empty for clarity. Below, in section 3.2 and

---

[a] *Department of Chemistry, Imperial College London, UK; E-mail: ast14@ic.ac.uk, fbresme@imperial.ac.uk*
[b] *Unilever R&D Port Sunlight, Quarry Road East, Bebington, Wirral, CH63 3JW, UK.*
[c] *Department of Chemical Engineering, Imperial College London, UK.*

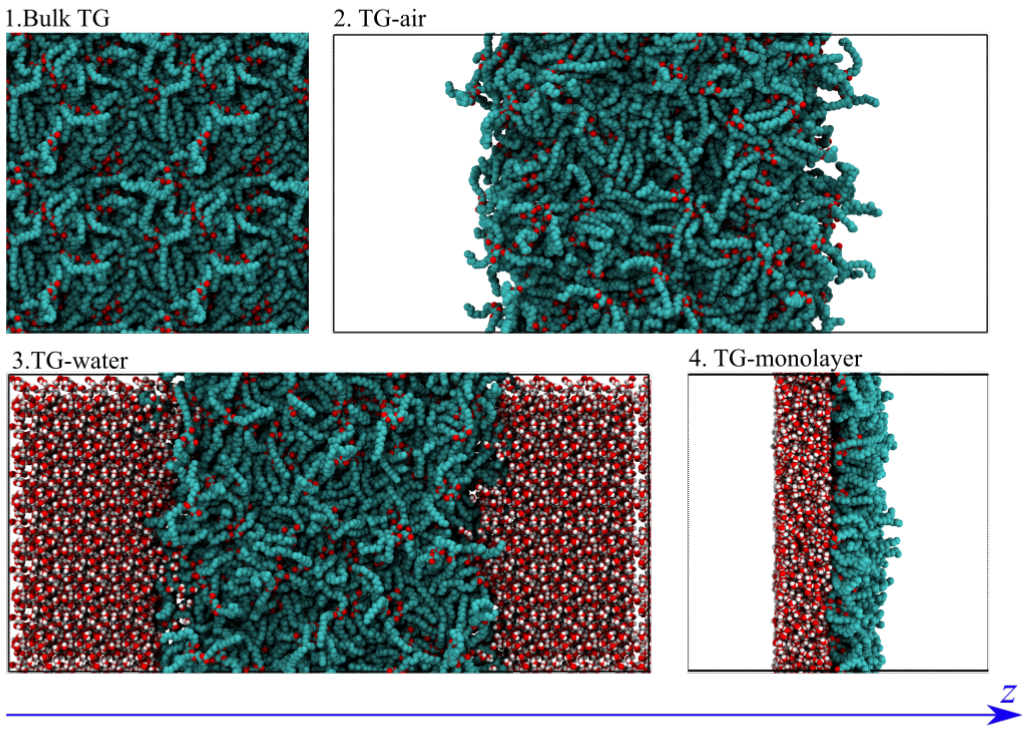

Fig. S1 1) Box of 512 triglyceride equilibrated for 20 ns; 2) the box is duplicated along *x* and *y* directions and void region is added along the *z* direction to generate 2 TG-air interfaces; 3) the void space is filled with 32126 water molecules to generate 2 TG-water interfaces; 4) Monolayer consisted of 122 TG molecules whose glycerol group was partially immersed in a water film with 9085 water molecules. The other surface of the water film was instead left free from TG.

Input configuration	N_{TG}	N_{water}	Ensemble	Production run time
Bulk TG	512	-	NPT	300 ns
TG-air	1024	-	NVT	100 ns
TG-water	1024	32126	NpT on z	200 ns
TG-monolayer	122	9085	NγT	at least 40 ns for each γ

Table S1 Main simulation parameters for the different input configurations. N_{TG} and N_{water} are the number of TG and water molecules, respectively. The production run time is the length of the simulation employed to compute the properties.

Fig. S7, we show the 4 regions overlapped to the 3D-plots of TG conformations for bulk-TG and TG-water interface.

2.2 Nearest neighbours

We present in Fig. S3 a representative snapshot of the bulk-TG configuration where two TG molecules, randomly selected, are highlighted in purple with their neighbouring molecules up to the first and second minimum of the C2-RDF. The position of the neighbours display the elongated shape of the head-group clusters. The position of the second broad minimum of the C2-RDF ($r \approx 1.6$ nm) can be related with the distance of C2 from the terminal carbon atom of the acyl chains. The three histograms in Fig. S4 show the distribution of these three C-C distances. The histograms are sharp and their maxima correspond to a C-C distance of ≈ 1.6 nm.

2.3 Independent initial configuration

To confirm the robustness of our results we repeated the bulk-TG simulations starting from an independent initial configurations. This configurations was generated by heating up our system to an high temperature ($T_H = 400$ K) followed by a slow cooling of the system down to the chosen working temperature, $T = 310$ K, with the simulated annealing technique, with the protocol described below. We took as initial configuration an equilibrated bulk-TG at the end of the production-run and set its temperature equal to T_H, leaving the system to equilibrate in the *NPT* ensemble for 100 ns. Then, we slowly cooled it down, following the simulated annealing procedure, by dynamically changing the reference temperature used in the thermostat algorithm, from T_H to 310 K during a 50 ns window. The resulting configuration was equilibrated for an additional 50 ns. A production run of 100 ns followed this equilibration procedure. We present in Fig. S5 the evolution of the system temperature (on the left-hand *y* axis) and the number of glycerol group clusters (right-hand *y* axis) obtained

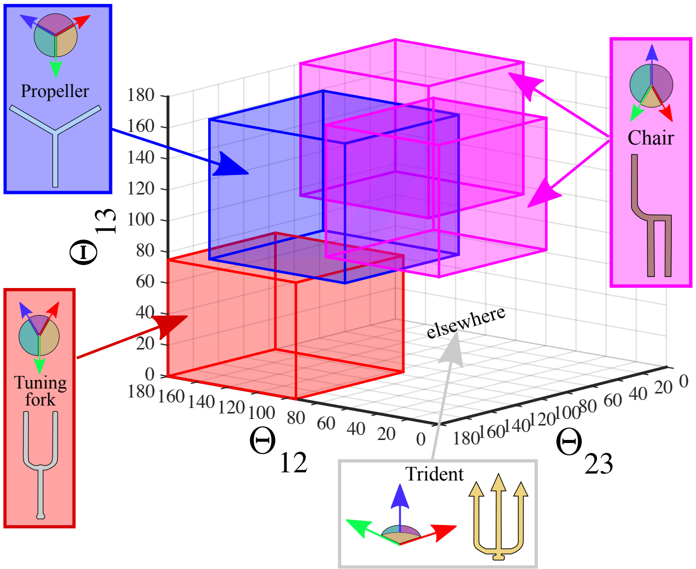

Fig. S2 Subdivision of the angles phase space into four conformations. The coloured cubes highlight regions assigned to the propeller (blue), the tuning fork (red) and the chair (magenta) conformations. In the remaining region the conformations were assigned to the trident.

with the voronoi algorithms described in the Methods section. The two insets are two representative simulation snapshots (at the beginning and the end of the simulated annealing equilibration) highlighting the shape of the clusters. This results confirm the evolution of the system from several small clusters to a single percolating network. The number of clusters keeps oscillating between 3 and 1 in the following 100 ns of production run, with one of the cluster involving almost all the TG headgroups (always over 80%).

3 TG-Water interface

3.1 Bulk-TG conformation analysis

The conformation analysis for bulk TG water is reported in Fig. S6. The distribution of the angles formed by the relative direction of pairs of chains, θ_{ij}, is represented in the three histograms in Fig. S6-left. Two of the angles are equivalent by symmetry (specifically θ_{12} and θ_{23}) and display a similar distribution in phase space as expected, with a maximum at about 140°. The θ_{13} distribution, instead, presents a maximum for lower angles ($\approx 50°$). The energetically allowed regions for TG conformations, expressed in terms of θ_{12}, θ_{23} and θ_{13} are represented in Fig. S6-right, where each circle represents the average conformation of one TG molecule. The size and the colour of the circles are proportional to the density of their occurrence in 3D-space. The colour bar above the graph gives a measure of the local numeric density of TG conformations inside a cubic mesh of side, $\delta\theta$, equal to 20° (corresponding to the mesh-grid of Fig. S6-right). The areas of the diagram corresponding to the four representative TG conformations (described in main paper Fig. 2) are highlighted with schematic illustrations of the three angles in these conformations. Despite the wide angle distributions and the occurrence of several conformations, the analysis suggests that the most likely intra-molecular arrangement presents the two opposite tails (sn1 and sn3) pointing towards one direction and the central one (sn2) pointing in the opposite direction (as shown in the inset of Fig. S6-right), resembling the shape of a tuning fork. The bulk TG in water has a similar angle distribution to bulk TG.

Shape	%
Propeller	23.00
Tuning fork	43.34
Chair	16.23
Trident	17.53

Table S2 Probability of appearance of the different shapes for bulk-TG in TG-w configuration. Results are expressed in % over all the molecules far from the interface (whose C2 was further than 1.5nm from the interface).

3.2 Classification of the conformational 3D-space

We report in Fig. S7 the graphs of the 3D conformational space for Bulk-TG, interfacial TG in TG-water interface and Bulk-TG in TG-water interface, highlighting the four regions of classification for the 4 shapes described in section 2.1. From the picture we can clearly observe the differences between the interfacial TG molecules, which preferentially assume an open trident shape and the bulk-TG molecules which are preferentially arranged as a tuning fork.

4 TG monolayer

4.1 Lateral radial distribution function

The long-range order in the lipid-lipid in-plane radial distribution function within the monolayer can be used to detect the transition from a liquid expanded phase to liquid condensed phase, as described in ref. 2 and 3. We computed the 2D lateral radial distribution function of the central carbon atom of the glycerol group (C2), RDF_{C2}, for different values of the surface pressure, Π. The different lines of Fig. S8 show RDF_{C2} for different values of Π, in $\mathrm{mN\,m^{-1}}$. Successive RDF functions have been shifted vertically by 0.05 units for greater clarity. Even at high values of the surface pressure, the RDF does not show long range oscillations, which would be indicative of the formation of a liquid condensed phase. This behaviour is reproduced across the different surface pressures investigated here (see Fig. S8). As discussed in the main paper, the double bonds of the TG tails confer on the TG molecules a wide conformation and the close packing of the liquid condensed phase is not reached.

4.2 Hysteresis

The presence of hysteresis and metastable states is revealed by realising a new set of simulations starting from the collapsed monolayer. Representative snapshots of the resulting configurations along the hysteresis curve (green curve in Fig.11 of the main paper) and the other curve (blue curve in Fig.11 of the main paper) are presented in Fig. S9. The monolayer is able to reorganise in a stable configuration for surface pressures, $\Pi \leq 12\,\mathrm{mN\,m^{-1}}$. Above this threshold the monolayers in the hysteresis curve (second col-

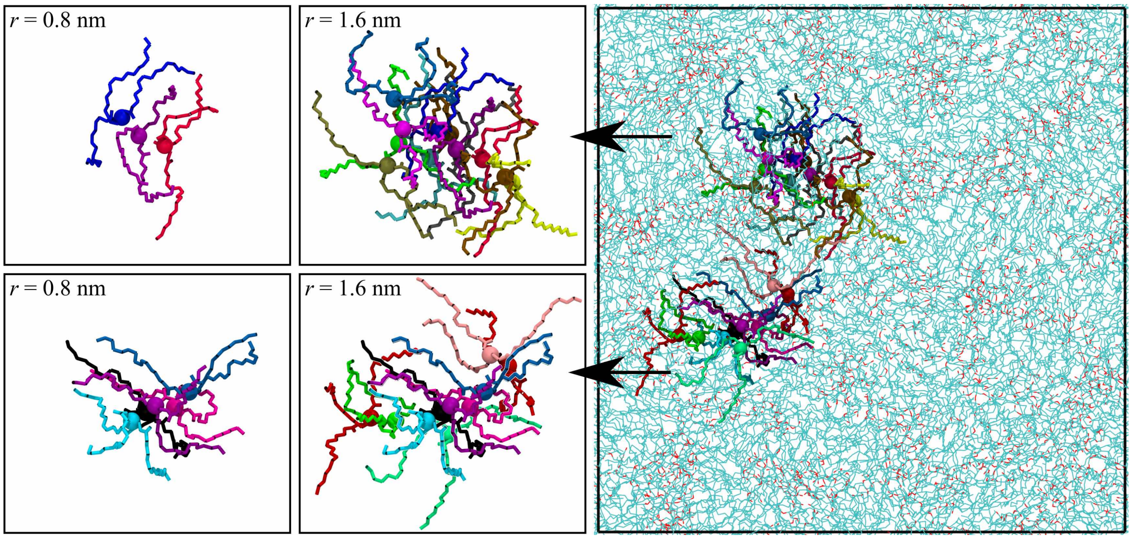

Fig. S3 Two representative TG molecules (in purple) and their neighbours are highlighted in the TG-bulk phase. The snapshots on the left show the nearest neighbours up to the first ($r \approx 0.8\,\mathrm{nm}$) and second ($r \approx 1.6\,\mathrm{nm}$) minimum of the c2-RDF.

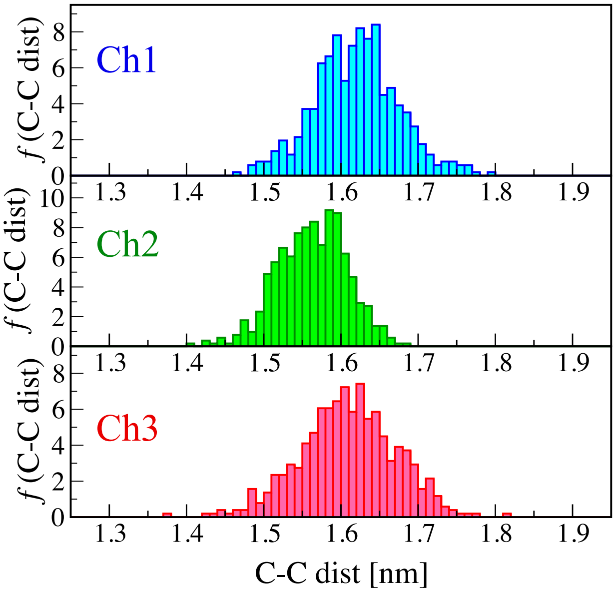

Fig. S4 Histograms of the distances between C2 (central carbon atom of the glycerol group - labelled in main paper) and the three terminal carbon atoms of acyl chains Ch1 (top), Ch2 (middle) and Ch3 (bottom).

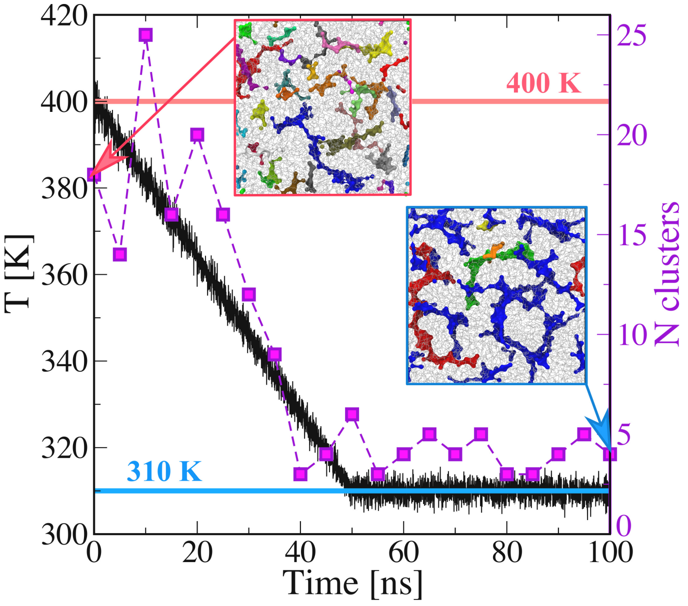

Fig. S5 Evolution of the average temperature (left-hand *y* axis) and number of clusters (right-hand *y* axis) with time, during the simulated annealing protocol (SA). The two insets illustrate the size and the number of clusters before and after the SA equilibration

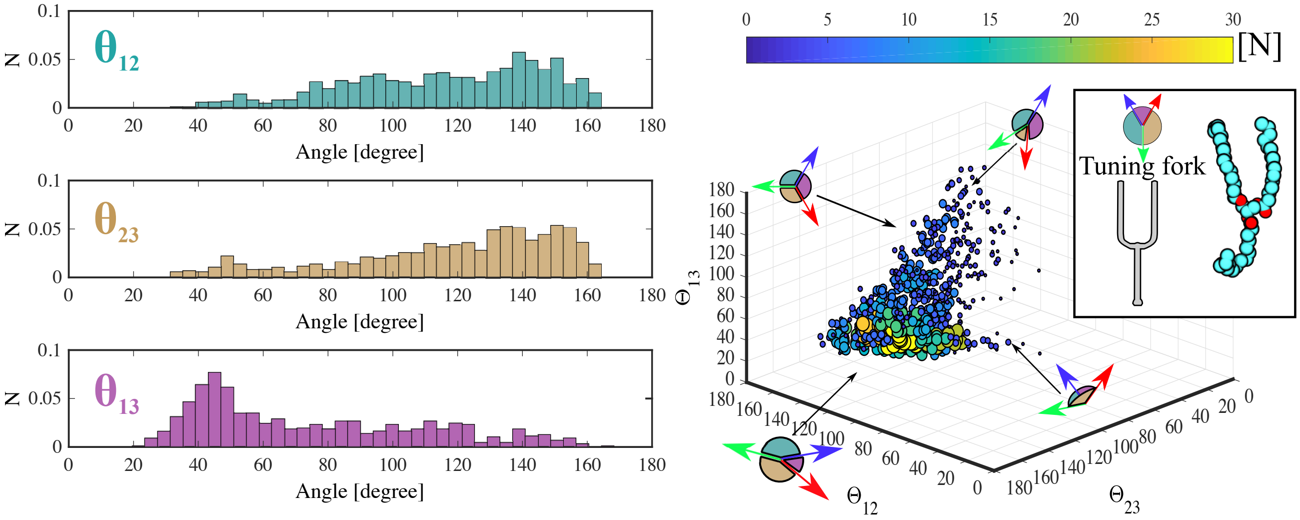

Fig. S6 Analysis of the intra-molecular TG-conformations. (Left) The three histograms represent the distributions of the angles, θ_{ij}. From top to bottom: θ_{12}, θ_{23} and θ_{13}. (Right) 3D distribution of triglyceride conformation as a function of the three angles described by the mutual orientation of the chains: θ_{12}, θ_{23} and θ_{13}. Each circle corresponds to the average conformation of a TG-molecule in the 3D space. The colour and size of the circles reflects the number density probability of each conformation, using a mesh-grid with $d\theta = 20^\circ$. The correspondence between colour and number density is given in the colour bar above the graph.

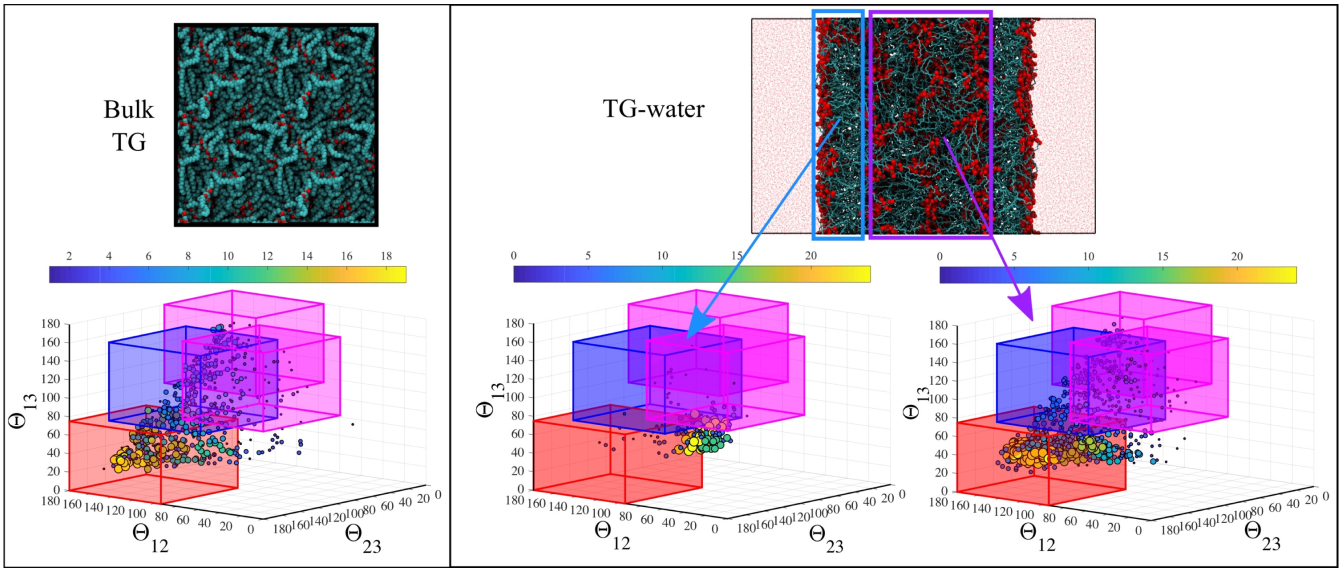

Fig. S7 From left to right: 3D distributions of triglyceride conformations as a function of the three angles, θ_{12}, θ_{23} and θ_{13}, for BULK-TG, interfacial TG at the TG-water interface and Bulk-TG at the TG-water interface. The 4 regions used for assigning the configurations to one of the 4 TG-shapes described in Section 2.1 are highlighted in the graphs with the same colour-code of Fig.S2: red for the *tuning fork*, blue for the *propeller*, magenta for the*chair* and elsewhere for the *trident*.

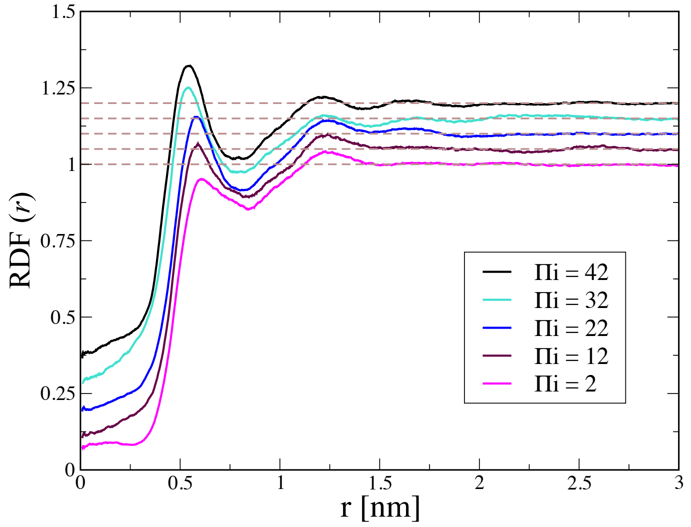

Fig. S8 Lateral radial distribution functions, *rdf*(r), of the central carbon atom of the glycerol group - C2 in the main paper, for different values of surface pressure expressed in $\mathrm{mN\,m^{-1}}$. The RDF have been shifted upwards by 0.05 units along the y-axis to enable a better comparison of the different curves.

umn of Fig. S9) are not able to rearrange themselves, with some of the triglyceride molecules located far from the main water interface, forming an inverse micellar structure.

4.3 Vapour phase transition

Metastable states can exist when the value of the surface tension, Π, is lower than 0, due to the required activation time for the monolayer transition to nucleate the vapour phase. The characteristic time of the transition to the vapour phase can be assessed by computing the time required for the area per lipid to diverge.

The area per lipid, $A_L(t)$, is defined by

$$A_L = \frac{\langle L_x(t) \times L_y(t) \rangle}{N_{TG}},$$

where $L_x(t) \times L_y(t)$ is the area of the simulation box at time t, and N_{TG} is the number of TG molecules. The curves in Fig. S10 show the evolution of A_L for several values of Π. For very negative values of Π, such as $-18\,\mathrm{mN\,m^{-1}}$ - dark green curve in Fig. S10, the transition to the vapour phase appears after a few nanoseconds. The closer the surface pressure is to $0\,\mathrm{mN\,m^{-1}}$, the longer the time to observe the transition. At $\Pi = -11\,\mathrm{mN\,m^{-1}}$ the transition happens after $\approx 20\,\mathrm{ns}$. At $\Pi = -2\,\mathrm{mN\,m^{-1}}$ a time longer then 20 ns would be required for the transition to take place.

References

1 R. W. Corkery, D. Rousseau, P. Smith, D. A. Pink and C. B. Hanna, *Langmuir*, 2007, **23**, 7241–7246.
2 D. Mohammad-Aghaie, E. Mace', C. A. Sennoga, J. M. Seddon and F. Bresme, *Journal of Physical Chemistry B*, 2010, **114**, 1325–1335.
3 D. Mohammad-Aghaie and F. Bresme, *Molecular Simulation*, 2016, **42**, 391–397.

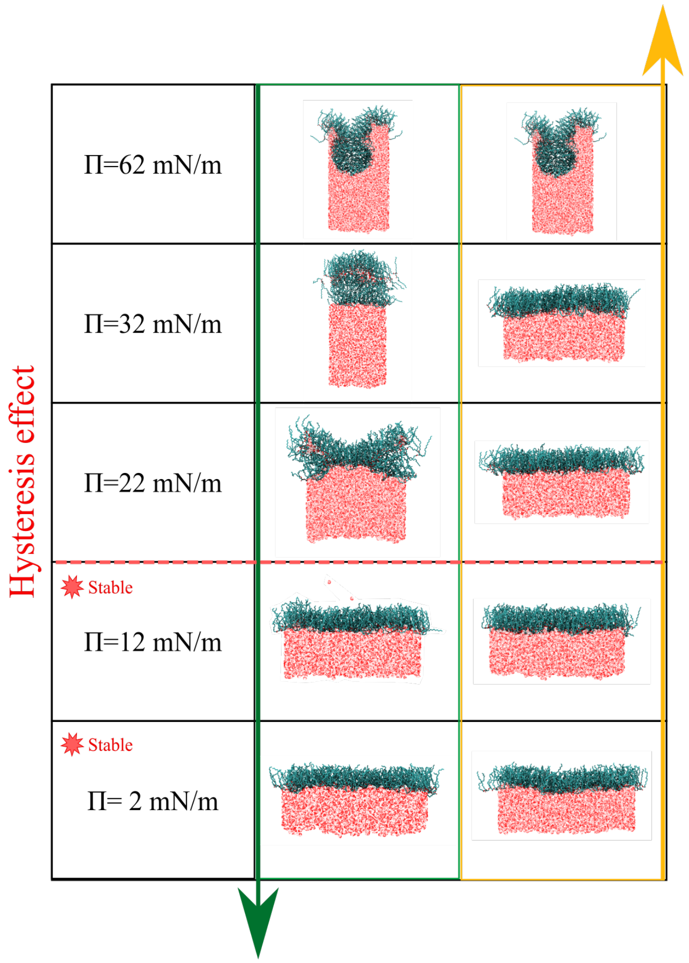

Fig. S9 Representative monolayer configurations at different surface pressures, Π. The second column (in green) corresponds to the configurations relative to the hysteresis curve, with initial area,$A_L0 = 34\,\text{Å}$. The third column corresponds to the configurations derived by an initial configuration with initial monolayer area $A_L0 = 110\,\text{Å}$. The threshold of stability ($\Pi > 12\,\mathrm{mN\,m^{-1}}$) is highlighted with a red line.

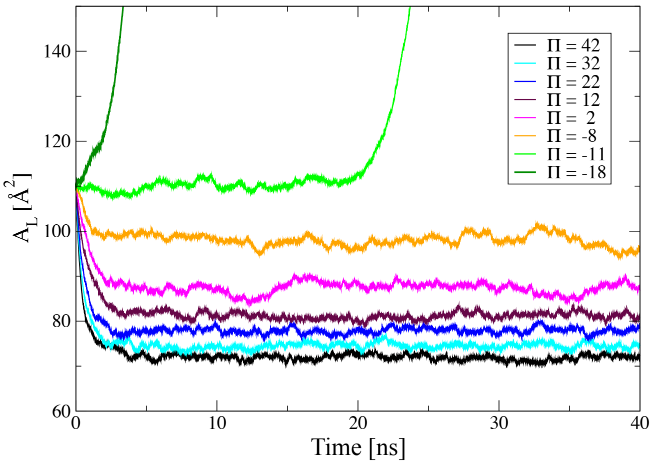

Fig. S10 Evolution of the area per lipid, A_L, with time. Different lines correspond to different surface pressures in $\mathrm{mN\,m^{-1}}$.